PERGAMON

Mechanism and Machine Theory 35 (2000) 99–115

MECHANISM AND MACHINE THEORY

www.elsevier.com/locate/mechmt

Limit positions of compliant mechanisms using the pseudo-rigid-body model concept

Ashok Midha[a], Larry L. Howell[b,*], Tony W. Norton[c]

[a]*Department of Mechanical and Aerospace Engineering and Engineering Mechanics, University of Missouri—Rolla, Rolla, MO, 65409-0050, USA*

[b]*Mechanical Engineering Department, Brigham Young University, Provo, UT, 84602-4138, USA*

[c]*Eastman Chemical Company, Kingsport, TN, 37662, USA*

Received 6 April 1998; received in revised form 22 October 1998

Abstract

Mechanisms which gain some or all of their motion from the relative flexibility of their members rather than from rigid-body joints alone are called compliant mechanisms. Determination of a compliant mechanism's kinematic mobility, including its degrees of freedom and limit positions, is complicated by geometric nonlinearities due to large deflections and the dependency of deflection on the placement and magnitude of applied loads. This paper introduces a method for determining the limit positions of compliant mechanisms for which an appropriate pseudo-rigid-body model may be created.

1. Introduction

Compliant mechanisms gain some or all of their motion from the relative flexibility of their members rather than from rigid-body joints alone. Two example compliant mechanisms are illustrated in Fig. 1.

The popularity of compliant mechanisms is expected to grow since the addition of compliance allows the designer greater freedom in the number of possible solutions for a given problem. However, this design freedom is often offset by difficulties encountered in the analysis of the compliant members. Often, compliant members undergo large deflections, and thus

* Corresponding author. Tel.: +1-801-378-2625; fax: +1-801-378-5037.
E-mail address: lhowell@et.byu.edu (L.L. Howell)

0094-114X/00/$ - see front matter
PII: S0094-114X(98)00093-7

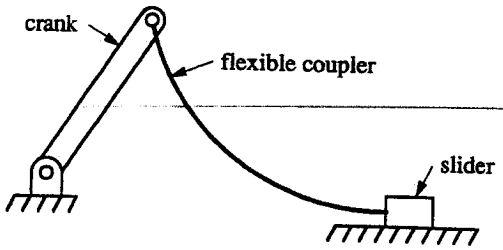

(a)

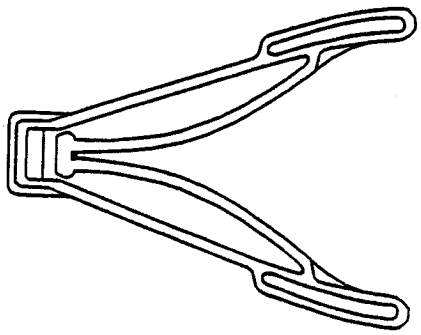

(b)

Fig. 1. (a) A partially compliant slider–crank mechanism, and (b) a fully compliant crimping tool.

nder the analysis nonlinear. Also, because the analysis requires a sound knowledge of both kinematics and solid mechanics, much of the intuition that is gained from experience in only one of these areas can be misleading. Unlike traditional rigid-body mechanisms, the displacements of a compliant mechanism can be highly dependent upon the applied loads, thereby adding a greater complexity to the analysis.

The pseudo-rigid-body model is one tool now available to simplify the analysis and design of compliant mechanisms. Such a model approximates a compliant mechanism by an appropriate, equivalent rigid-body mechanism. This allows the wealth of rigid-body mechanism technology to be applied to the analysis of compliant mechanisms.

Determining the number and form of inputs required to obtain a desired motion is critical in the analysis and design of mechanisms. Knowledge of the physical limits of a mechanism's motion is also usually required to obtain an acceptable mechanism design. The calculation of kinematic limits for compliant mechanisms may be difficult to determine considering that they are dependent not only on relative link lengths and geometry, but also on member stiffness, and the location and magnitude of applied loads. This work proposes the use of the pseudo-rigid-body model of a compliant mechanism to approximate the mechanism's limit positions. Several demonstrative examples are introduced to illustrate the concepts presented. These developments are proceeded by a brief review of the pseudo-rigid-body model concept.

2. Pseudo-rigid-body model

Salamon [1] introduced a methodology for compliant mechanism design that used a pseudo-rigid-body model of the compliant mechanism with the compliance modeled as torsional and linear springs. These models are much easier to analyze than idealized models which require finite element or elliptic integral solutions. Pseudo-rigid-body models generally have closed-form displacement and force equations that allow the designer to more easily see the effects of parameters on mechanism design. The most important attribute of the pseudo-rigid-body model is that it significantly simplifies the design process.

Howell and Midha [2] presented a model for flexible segments that are small in length compared to the adjacent rigid segments. This model consists of a pin joint at the center of the segment, and a torsional spring to represent the resistance.

Howell and Midha [3] studied the effect of nonfollower end forces on a simple fixed–pinned segment shown in Fig. 2. The horizontal and vertical coordinates of the deflected beam end (Fig. 2) are defined as a and b, respectively.

The results were used to create a rigid-body model of the beam shown in Fig. 3; this model will be called the "pseudo-rigid-body model" of the beam. Here, the beam has been replaced by a link with a characteristic pivot located at a length γl from the free end of the beam. Values for the characteristic radius factor are found in [3].

The beam end angular deflection, θ_0, may be written as

$$\theta_0 = c_\theta \Theta \tag{1}$$

where c_θ is a constant, called the characteristic angle coefficient, and Θ is the angular displacement of the pseudo-rigid-body link and is called the characteristic angle. Limits for the above approximations are given by

$$\theta_0 < \theta_{0\,\max} \cong 0.85\phi = 0.85 \tan^{-1}(1/-n); \quad -5.0 < n < 10 \tag{2}$$

where $\theta_{0\max}$ is the maximum allowable end angle of the beam, and n is the ratio of the vertical component of the load (P) to the horizontal component of the load. These limits may also be

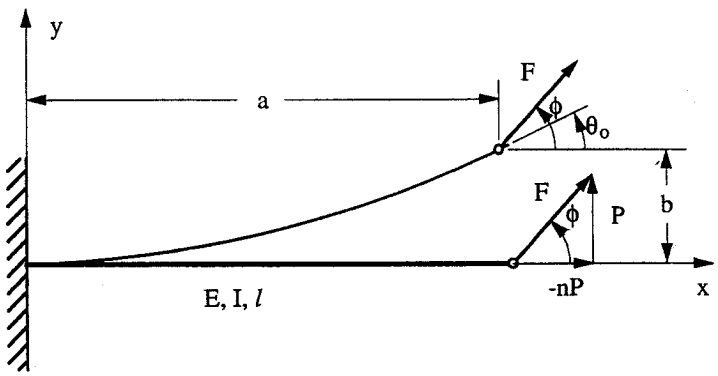

Fig. 2. Simple fixed–pinned segment.

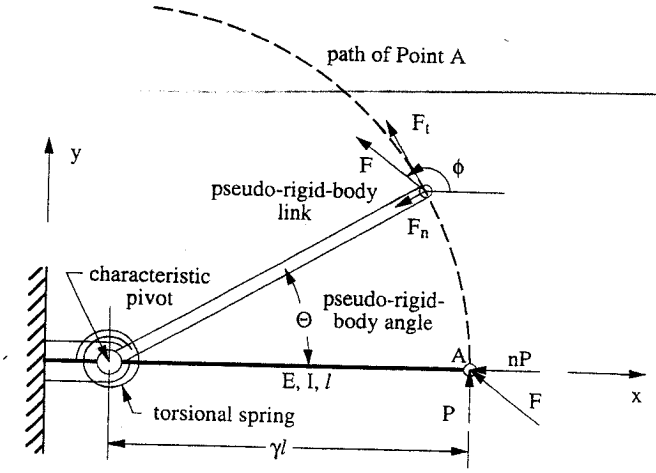

Fig. 3. Pseudo-rigid-body model for a functionally binary, simple, fixed–pinned segment.

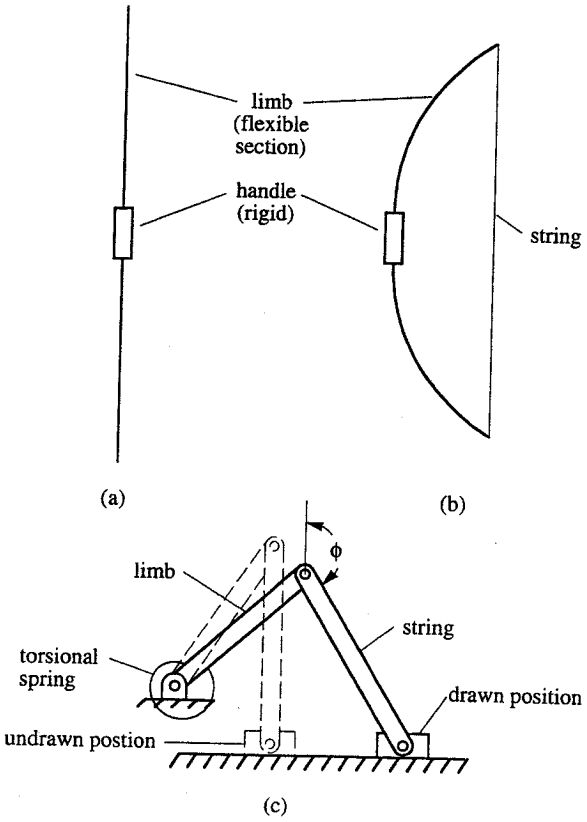

Fig. 4. A longbow in its (a) unstrung and (b) strung positions and (c) its pseudo-rigid-body model.

expressed in terms of the pseudo-rigid-body angle, Θ, as given by [4]

$$\Theta<\Theta_{max} \cong 0.7\phi = 0.7 \tan^{-1}(1/-n); \quad -5.0<n<10.0 \tag{3}$$

where Θ_{max} is the maximum allowable pseudo-rigid-body angle.

Force–deflection relationships in terms of the nondimensionalized load, $\alpha^2 = Pl^2/EI$, and the pseudo-rigid-body angle, Θ were also presented in [3]. Norton [4] and Howell et al. [5] proposed a "stiffness coefficient" which relates the pseudo-rigid-body angle, Θ, and the nondimensionalized transverse load, α_t^2, i.e.

$$\alpha_t^2 = K_\Theta \Theta \tag{4}$$

where

$$\alpha_t^2 = \frac{F_t l^2}{EI} \tag{5}$$

and F_t is the tangential component of the applied nonfollower force F shown in Fig. 3. The stiffness coefficient, K_Θ, is therefore the stiffness of the torsional spring at the characteristic pivot shown in Fig. 3. Values of K_Θ for various end force loadings are found in [4,5].

A novel example of the use of the large-deflection parameterization and compliant mechanism concepts introduced herein is the archer's longbow. The longbow has a significant place in military history, hunting, sports and recreation [6]. The longbow has remained an important classical problem, particularly in light of the development in materials and analysis methods.

Fig. 4 shows a longbow in its unstrung (Fig. 4a) and strung (Fig. 4b) positions. Using the pseudo-rigid-body model for the flexible section of the bow and making use of its symmetry, the strung bow can be modeled as a slider–crank mechanism, as shown in Fig. 4c. The bow string, represented by the coupler, is obviously a two-force member. So, when the coupler angle is known, n may be found from:

$$n = -\cot\phi \tag{6}$$

where n is the ratio of the axial to transverse force (F_n/F_t) and ϕ is as shown in Fig. 4c.

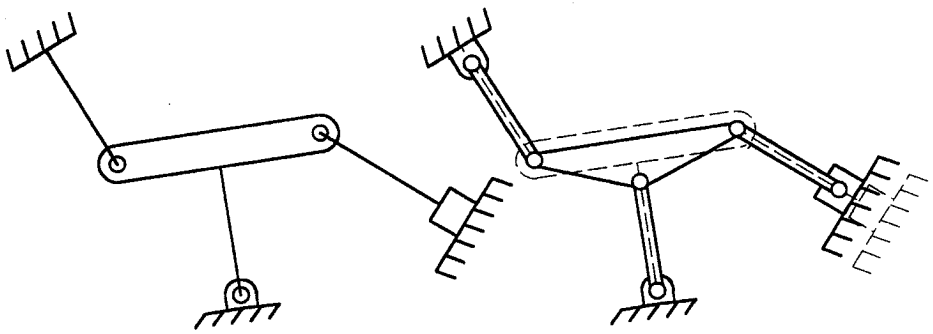

Fig. 5. Example compliant mechanism and its pseudo-rigid-body model.

The kinematics and the required input and reaction forces may now be readily evaluated by incrementing the displacement coordinate of the slider, obtaining the deflection, and calculating the resulting reaction loads. This process is continued until the deflections and reactions are found for a satisfactory range of slider travel.

Another example of a compliant mechanism is given in Fig. 5a. Its resulting pseudo-rigid-body model (shown in Fig. 5b) may be used to analyze the behavior of the mechanism.

3. Four-bar-type compliant mechanisms

The simplicity and versatility of a rigid-body four-bar mechanism has made it one of the most widely used mechanisms. A large part of mechanism theory has been devoted to the discussion of four-bar mechanisms [7]. It is therefore reasonable to assume that many applications of compliant mechanisms will involve those mechanisms whose pseudo-rigid-body models resemble four-bar mechanisms.

Consider the mechanism shown in Fig. 6a. The pseudo-rigid-body model in Fig. 6b is used

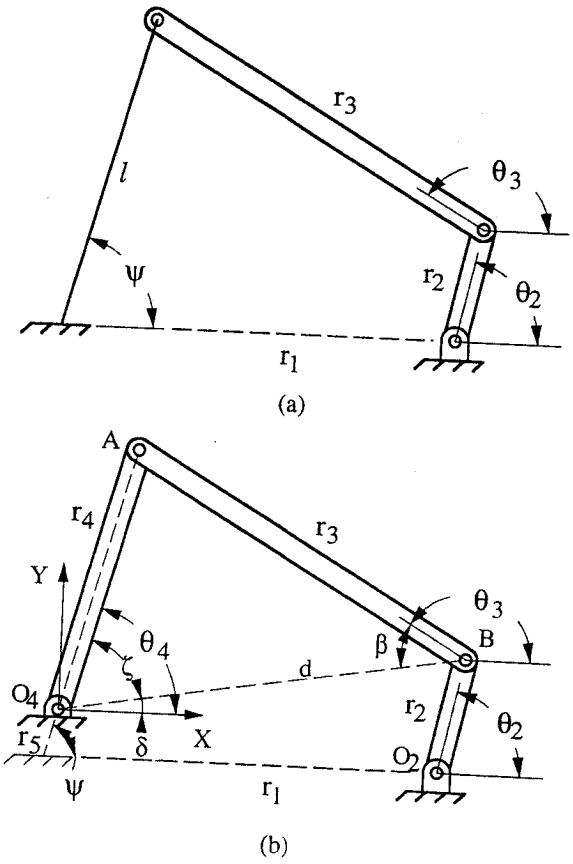

Fig. 6. (a) A compliant mechanism; and (b) its pseudo-rigid-body model.

to derive equations for obtaining the displacement of the mechanism. The flexible member is modeled as shown, and

$$r_4 = \gamma l \tag{7}$$

$$r_5 = (1-\gamma) l \tag{8}$$

$$X_B = r_1 + r_2 \cos\theta_2 - r_5 \cos\Psi \tag{9}$$

$$Y_B = r_2 \sin\theta_2 - r_5 \sin\Psi \tag{10}$$

where X_B and Y_B are the x and y coordinates of point B, respectively, r_i and θ_i are the length and angle of link i, respectively, and Ψ is the angle of the flexible segment in its undeformed configuration. The displacement calculations may now be accomplished using standard rigid-body mechanism analysis techniques.

4. Limit positions of compliant mechanisms

The mobility of planar rigid-body mechanisms has been well explored. Many of these studies are centered on the triangle inequality concept. Midha et al. [8] use a graphical interpretation of the triangle inequality concept to study the mobility conditions for planar linkages. Norton et al. [9–11] extend this method to show solution spaces for synthesis problems in which the mobility region and type of mechanism are given. Norton et al. [10] also use the triangle inequality concept to categorize Non-Grashofian four-bar mechanisms according to their mobility. Ting [12] extended the triangle inequality concept to study the mobility of single-loop, n-bar linkages. He develops what is referred to as the theorem of assemblability and the theorem of revolvability which degenerate to the triangle inequality concept for the four-bar mechanism.

A limit position of a rigid-body mechanism occurs when a parameter used to measure the motion of the mechanism reaches an extreme value. For example, consider the mechanism of Fig. 7. This mechanism is said to have reached a limit position when angle θ_4 has reached its

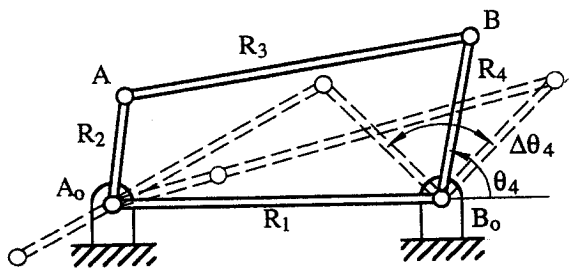

Fig. 7. Limit positions of a rigid-body four-bar mechanism.

maximum or minimum value. The possible values for angle θ_4 between its limits define the mobility region of the mechanism, given by $\Delta\theta_4$.

In general, infinite degrees of freedom are needed to describe the motion of a compliant member. These degrees of freedom may or may not reach extreme values coincidentally. Therefore, there is no one position at which the compliant member can be considered to be at a limit position. Furthermore, the extent of the motion of a compliant member is highly dependent upon the applied forces. Therefore, the compliant member can have different limit positions for different input forces.

The pseudo-rigid-body model of a compliant member reduces the infinite degrees of freedom of that member to a finite number. Therefore, mobility concepts similar to that used in analyzing rigid-body mechanisms may be used for compliant mechanisms with appropriate changes to account for compliance.

Once a suitable kinematic model of a compliant mechanism is found, we may study the mobility of this model. The kinematic mobility of a compliant mechanism is the mobility of the kinematic model of that mechanism where no restrictions have been placed on the location of input forces, except those necessary for the establishment of the kinematic model. It should be noted that kinematic mobility may be defined for a mechanism only if a valid kinematic model can be established for the mechanism.

5. Functionally binary, simple, fixed–pinned segment

Consider the simple fixed–pinned segment in Fig. 2. If the only points of force application are at the ends of the segment, then the segment is functionally binary [13]. The kinematic model for this segment (Fig. 3) is valid for values of ϕ between zero and 180°, and for values the pseudo-rigid-body angle, Θ, less than approximately 125°. We may study the mobility of the kinematic model first, and then interpret the implications of its results for the actual compliant segment. The kinematic model of a simple, fixed–pinned segment is valid only when

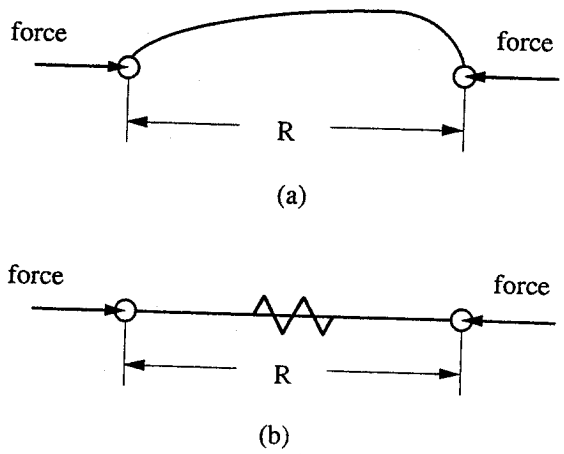

Fig. 8. (a) A functionally binary, pinned–pinned segment; and (b) its kinematic model.

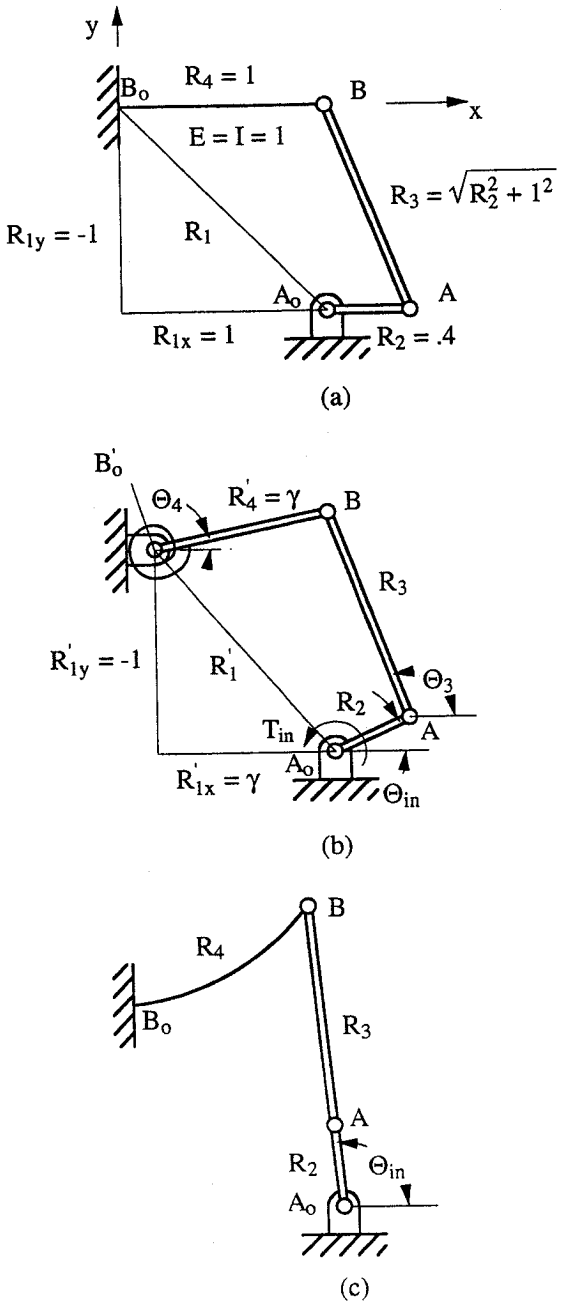

Fig. 9. (a) Mechanism initial position; (b) its pseudo-rigid-body model; and (c) toggle position.

the pseudo-rigid-body angle, Θ, is less than 70% of the angle of the applied force, ϕ, as given by Eq. (3). A consequence of this limitation is that Θ must be less than approximately 125°. This condition will be neglected when considering kinematic mobility. The implications of Eq. (3) may be taken into account when determining the "structural mobility" of the mechanism

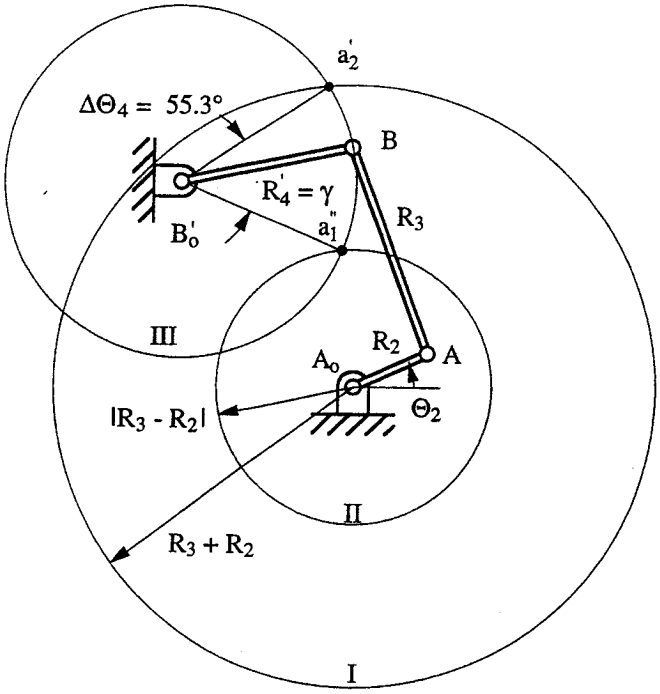

(a)

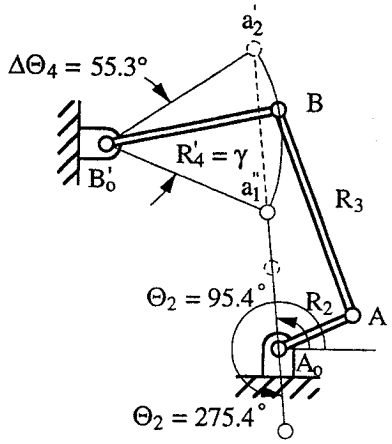

(b)

Fig. 10. Construction of example 1.

given
125°.
of Eq.
anism

[4]. The structural mobility of a mechanism takes into account prescribed boundary conditions of force and displacement. A structural limit is reached, for example, when very small displacements occur for large increases in input forcing.

6. Functionally binary, pinned–pinned segment

A functionally binary, pinned–pinned segment is shown in Fig. 8a. A functionally binary

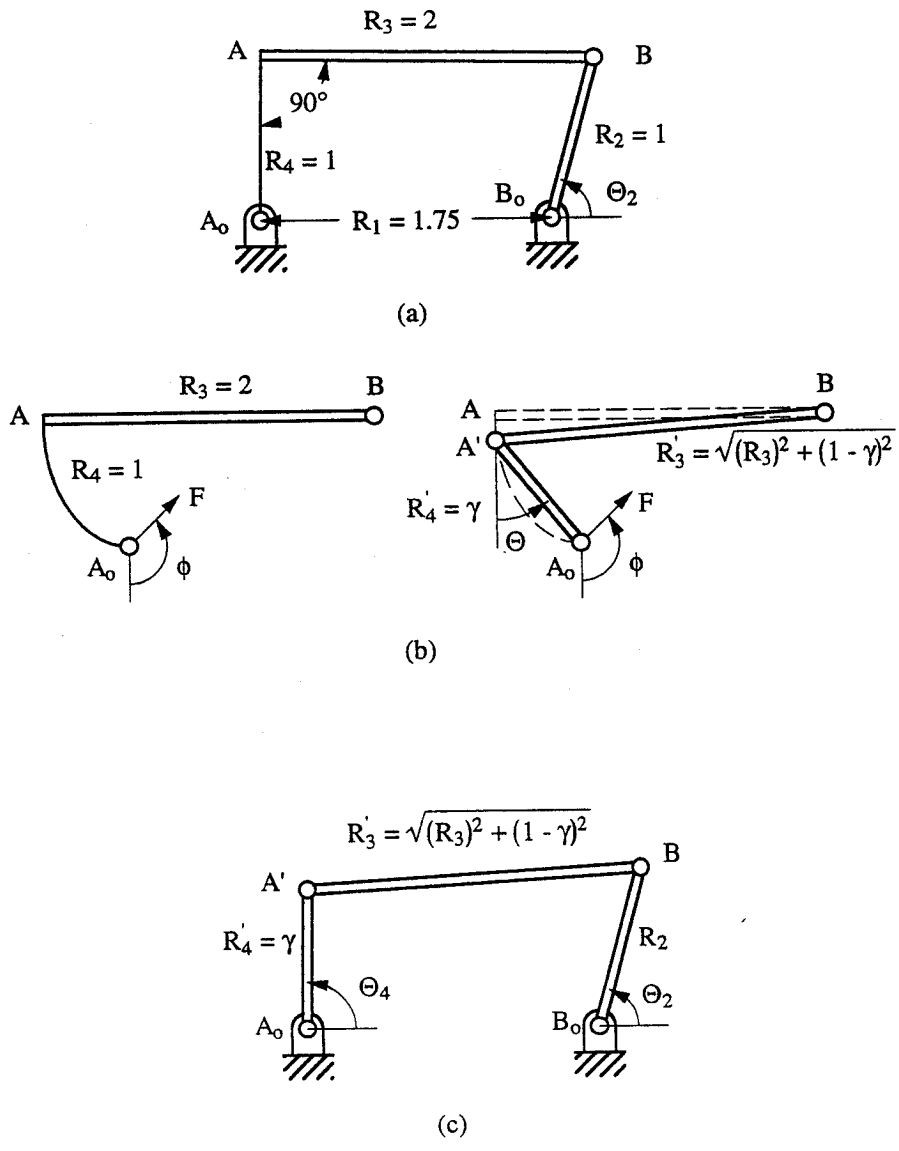

Fig. 11. Mechanism of example 2 and its kinematic model.

segment by definition assumes that all forces are applied at its two pins. A functionally binary, pinned–pinned segment is a two-force member, and will always act as an axially compliant segment; its kinematic model is shown in Fig. 8b. For kinematic mobility, the limits of this segment are assumed to be given as R^{max} and R^{min}, and the mobility region is described by ΔR.

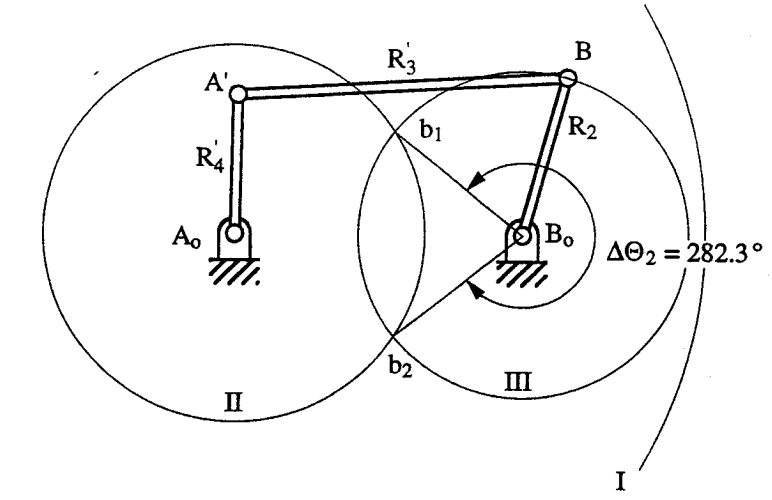

(a)

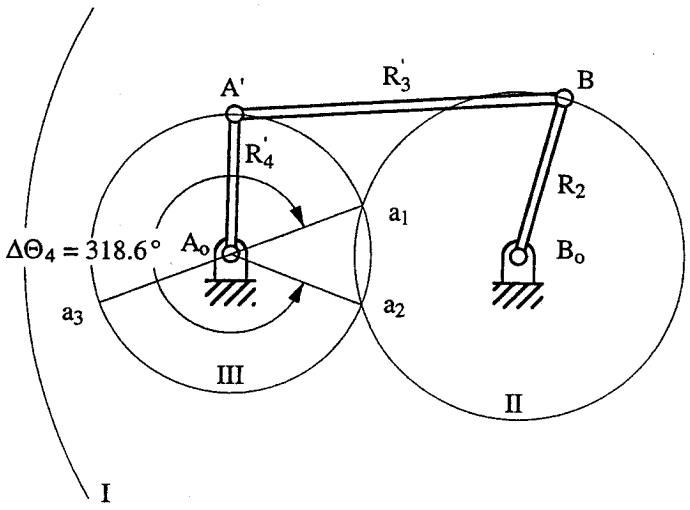

(b)

Fig. 12. Kinematic limits of the mechanism of example 2.

6.1. Example 1

Find the kinematic limits of the mechanism shown in Fig. 9a.

To simplify the kinematic model for this mechanism, the characteristic pivot location will be assumed to be constant during the motion of the mechanism. Howell and Midha [3] noted that as a rule of thumb γ is approximately equal to 0.85. Using this approximation, a kinematic model can be formed as shown in Fig. 9b. To determine the limit positions of this model, as shown by Midha et al. [8] three circles are drawn. The first circle (circle I), has a radius of $(R_3 + R_2)$ and a center point at A_0. Circle I represents the maximum allowable distance between the points B and A_0 as constrained by links R_3 and R_2 (Fig. 10a). The second circle (circle II) of radius $|R_3 - R_2|$ and with center point at A_0, represents the minimum allowable distance between the points B and A_0 as constrained by links R_3 and R_2. The third circle (circle III) of radius R_4' and with center point at B_0', represents the path of point B as constrained by link R_4'.

The intersections of circles I and II with circle III at points a_1'' and a_2' define the limit positions of link R_4'. The range of mobility of link R_4', $\Delta\Theta_4$, is measured to be 55.3°. Norton et al. [10] showed that when both circles I and II intersect circle III link R_2 is a crank and can therefore revolve about the base.

Link R_4' is a rigid-body representation of the compliant segment; its mobility range is of

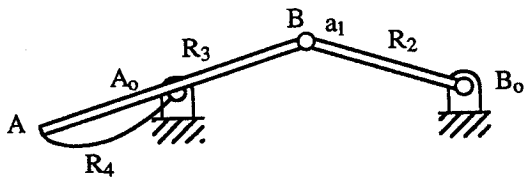

(a)

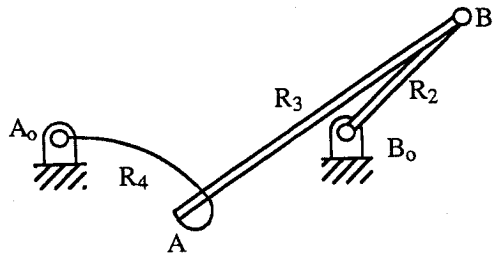

(b)

Fig. 13. (a) Acceptable and (b) unacceptable positions for the mechanism of example 2.

interest because it would then allow one to find the values of Θ_2 corresponding to its kinematic limit positions. In Fig. 10b, these values are measured as 95.4° and 275.4°. The configuration the mechanism when Θ_2 is 95.4° is shown in Fig. 9c. At this position, zero input torque is required for the forcing conditions. Also, when Θ_2 is 275.4°, the required input torque is zero.

6.2. Example 2

Determine the kinematic limits of the compliant mechanism shown in Fig. 11a which is at stable equilibrium.

As before, the characteristic pivot location is assumed to be fixed, and the value of γ to be 0.85. The resulting kinematic model of link R_3R_4 (A_0AB) is shown in Fig. 11b. The kinematic model of this mechanism is shown in Fig. 11c. As before, three circles are drawn to determine the mobility of link R_2 (Fig. 12a). Since circle II intersects circle III at points b_1 and b_2, and circle I does not, the kinematic model is Non-Grashofian [10], i.e. link R_4' is not a crank.

The mobility of link R_4' is determined in a similar manner as shown in Fig. 12b. The points of intersection a_1 and a_2 are the limit positions of the kinematic model, but in order to reach the position of the mechanism at which point A' is coincident with point a_2, the assumptions regarding the range of the kinematic model are invalid. The pseudo-rigid-body angle, Θ, shown in Fig. 11b must be less than approximately 125° for the kinematic model to be valid.

If we consider the position of the kinematic model where point A' is coincident with the point a_3, shown in Fig. 12b, the angle Θ is 90°. This is an acceptable value if the applied forces are such that Eq. (3) is not violated. At this position the mechanism will appear as in Fig. 13a.

As point A' (Fig. 12b) moves counter-clockwise from this position toward the kinematic limit at a_2, the angle Θ increases beyond 125°, and the mechanism reaches configurations such that shown in Fig. 13b. These are undesirable configurations, and the kinematic model of R_3R_4 is clearly invalid because the pseudo-rigid-body angle is greater than 180°. This example shows that the limit positions of a compliant mechanism cannot always be measured from the kinematic model alone.

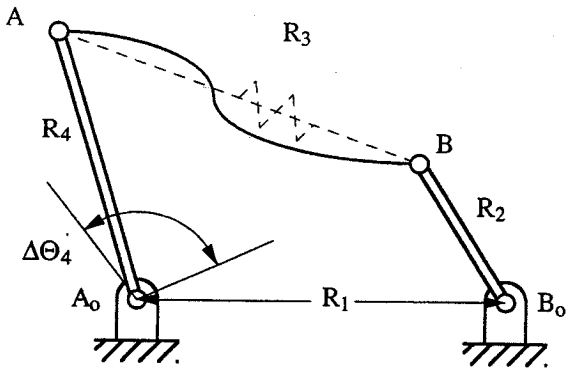

Fig. 14. A four-link, compliant mechanism with a functionally binary, pinned–pinned coupler link.

6.3. Example 3

Suppose a mechanism is to be constructed from three rigid links and one functionally binary, pinned–pinned link, as shown in Fig. 14. If the angle between the limit positions of link R_4, $\Delta\Theta_4$, is to be 60°, R_3^{max} is 2.5, R_3^{min} is 2.0, and R_4 is 1.5, then show the solution space for all mechanisms for which link R_2 is a crank.

Norton et al. [9] showed that for a specified value of $\Delta\Theta_4$ the base pivot B_0 must lie in the hatched region of Fig. 15 if link R_2 is to be a crank. This hatched region is referred to as the Grashofian region. To determine the effects of the given link length constraints, the limit positions of link R_4 are constructed for the given mobility angle, $\Delta\Theta_4$, as shown in Fig. 16. A base pivot location, B_0, meeting the given constraints exists (Fig. 16). For all solutions with base pivots B_0 to the right of base pivot A_0, the distance B_0a_1'' is the minimum possible distance between the points B_0 and A and is equal to $|R_3^{min}-R_2|$. Also, the distance B_0a_2' is the maximum possible distance between the points B_0 and A and is equal to $R_3^{max}+R_2$. For all possible solutions the sum of B_0a_1'' and B_0a_2' is $R_3^{max}+R_3^{min}$. The locus of all points meeting this requirement is an ellipse. The locus of all points on the ellipse that are in the Grashofian region comprise the complete set of B_0 locations that meet the problem specifications.

7. Conclusion

The pseudo-rigid-body model of a compliant mechanism has been briefly reviewed in this paper. The limit positions of compliant mechanisms have been investigated using the pseudo-rigid-body model and rigid-body mechanism analysis methods. This offers, for the first time, a simple method to approximate the kinematic limitations of compliant mechanisms.

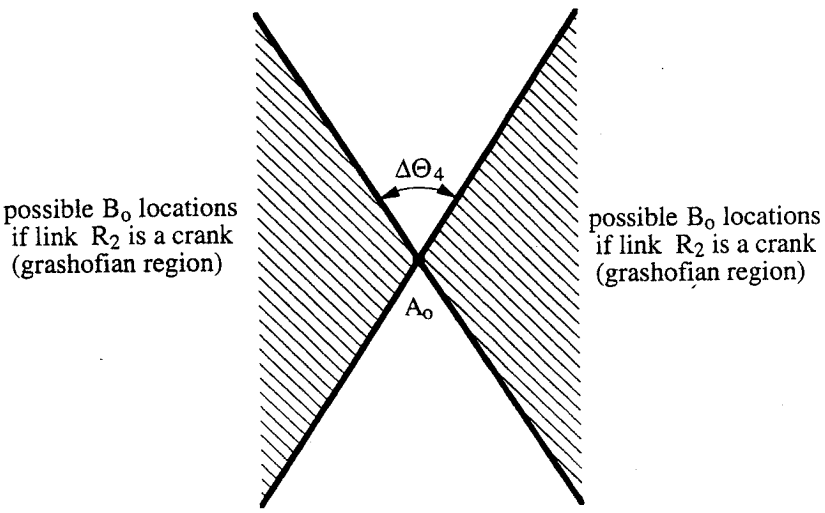

Fig. 15. Grashofian region for a given mobility angle.

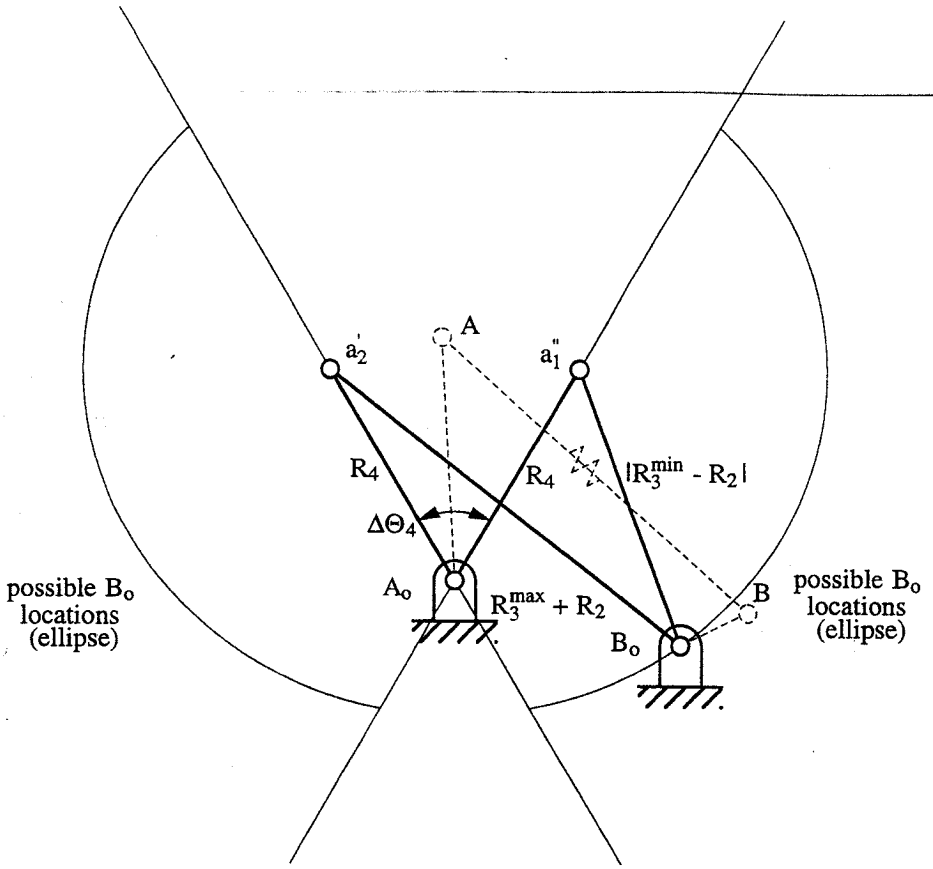

Fig. 16. Solution space for example 3.

Acknowledgements

The research support of the National Science Foundation, through NSF grant no. MSS-8902777, is gratefully acknowledged.

References

[1] B.A. Salamon, 1989 Mechanical advantage aspects in compliant mechanisms design. M.S. Thesis, Purdue University.
[2] L.L. Howell, A. Midha, A method for the design of compliant mechanisms with small-length flexural pivots, Journal of Mechanical Design 116 (1994) 280–290.
[3] L.L. Howell, A. Midha, Parametric deflection approximations for end-loaded, large-deflection beams in compliant mechanisms, Journal of Mechanical Design 117 (1995) 156–165.
[4] T.W. Norton, 1991 On the nomenclature and classification, and mobility of compliant mechanisms. M.S. Thesis, Purdue University.

[5] L.L. Howell, A. Midha, T.W. Norton, Evaluation of equivalent spring stiffness for use in a pseudo-rigid-body model of large-deflection compliant mechanisms, Journal of Mechanical Design 118 (1996) 126–131.
[6] E. McEwen, R.L. Miller, C.A. Bergman, Early bow design and construction, Scientific American (1991) 76–82.
[7] A.S. Hall Jr, Kinematics and linkage design, Waveland Press, Prospect Heights, IL, 1986.
[8] A. Midha, Z. Zhao, I. Her, Mobility conditions for planar linkages using triangle inequality and graphical interpretation, Journal of Mechanisms, Transmissions, and Automation in Design, Trans. ASME 107 (1985) 394–400.
[9] T.W. Norton, L.L. Howell, A. Midha, Graphical synthesis of a four-bar mechanism for specification of limit positions or transmission angle, in: Proceedings of the Second National Applied Mechanisms and Robotics Conference, Cincinnati, OH, November, 1991, 1991 Paper no. IIA-4.
[10] T.W. Norton, L.L. Howell, A. Midha, Graphical synthesis for limit positions of a four-bar mechanism using the triangle inequality concept, Journal of Mechanical Design 116 (1994) 1132–1140.
[11] T.W. Norton, L.L. Howell, A. Midha, On graphical synthesis techniques for planar four-bar mechanisms for limit positions and high performance, in: A. Erdman (Ed.), Modern kinematics: developments in the last forty years, Wiley, New York, 1993, pp. 87–95 Section 4.5.
[12] K.L. Ting, Mobility criteria of single-loop *N*-bar linkages, Journal of Mechanisms, Transmissions, and Automation in Design, Trans. ASME 111 (1989) 504–507.
[13] A. Midha, T.W. Norton, L.L. Howell, On the nomenclature, classification and abstractions of compliant mechanisms, Journal of Mechanical Design 116 (1994) 270–279.

. MSS-

, Purdue

al pivots,

n compli-

ms. M.S.